AD-A042 677 NAVAL WEAPONS CENTER CHINA LAKE CALIF F/G 4/2
ELECTROSTATIC INDUCTION PARAMETERS TO ATTAIN MAXIMUM SPRAY CHAR--ETC(U)
1976 J W CARROZ, P N KELLER

UNCLASSIFIED NL

1 OF 1

ADA042-677

END
DATE FILMED
8-77
DDC

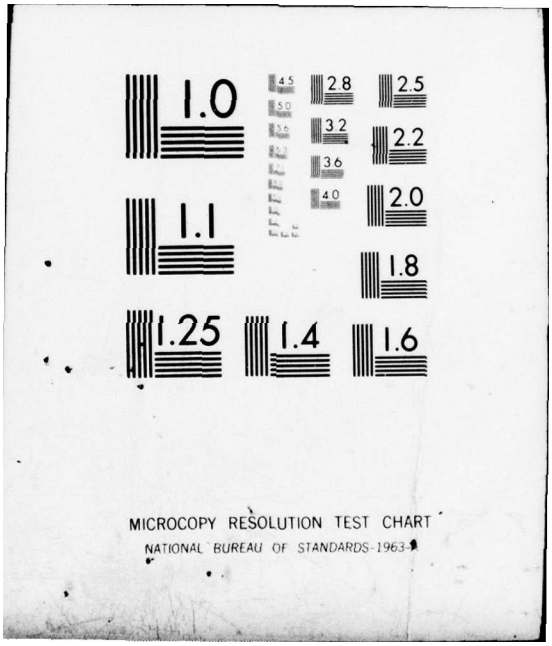
1.0
1.1
1.25
1.4
1.6
1.8
2.0
2.2
2.5
2.8
3.2
3.6
4.0
4.5
5.0
5.6
MICROCOPY RESOLUTION TEST CHART
NATIONAL BUREAU OF STANDARDS-1963-A

UNCLASSIFIED

SECURITY CLASSIFICATION OF THIS PAGE *(When Data Entered)*

REPORT DOCUMENTATION PAGE

READ INSTRUCTIONS BEFORE COMPLETING FORM

1. REPORT NUMBER

2. GOVT ACCESSION NO.

3. RECIPIENT'S CATALOG NUMBER

4. TITLE *(and Subtitle)*

Electrostatic Induction Parameters to Attain Maximum Spray Charge.

5. TYPE OF REPORT & PERIOD COVERED

6. PERFORMING ORG. REPORT NUMBER

7. AUTHOR(s)

John W. Carroz & Patrick N. Keller

8. CONTRACT OR GRANT NUMBER(s)

9. PERFORMING ORGANIZATION NAME AND ADDRESS

Naval Weapons Center
China Lake, California 93555

10. PROGRAM ELEMENT, PROJECT, TASK AREA & WORK UNIT NUMBERS

63207N; W3712;
W3712-000; 1602011F

11. CONTROLLING OFFICE NAME AND ADDRESS

Naval Weapons Center
China Lake, California 93555

12. REPORT DATE

1976

13. NUMBER OF PAGES

35

14. MONITORING AGENCY NAME & ADDRESS *(if different from Controlling Office)*

37 P.

15. SECURITY CLASS. *(of this report)*

Unclassified

15a. DECLASSIFICATION/DOWNGRADING SCHEDULE

16. DISTRIBUTION STATEMENT *(of this Report)*

Approved for public release; unlimited distribution.

17. DISTRIBUTION STATEMENT *(of the abstract entered in Block 20, if different from Report)*

18. SUPPLEMENTARY NOTES

Revision of 1975 article.

19. KEY WORDS *(Continue on reverse side if necessary and identify by block number)*

- Electrostatic spraying
- Maximum spray charge
- Electrostatic induction
- Fluid conductivity
- Fluid pressure

20. ABSTRACT *(Continue on reverse side if necessary and identify by block number)*

Laboratory experiments using sprays of charged drops were conducted to support a fog clearing program. Sprays from 1-gram per second hollow-cone industrial spray nozzles were induction charged to 5.7×10^{-6} coulombs per gram of spray. As the nozzle size was increased, the charge per unit mass of spray decreased. Increasing the airflow past the nozzle increased the charge on the spray. Increasing induction surface, fluid conductivity, and voltage increased the spray charge to a limit beyond which further increases

DD FORM 1 JAN 73 1473 EDITION OF 1 NOV 65 IS OBSOLETE S/N 0102-014-6601

UNCLASSIFIED

SECURITY CLASSIFICATION OF THIS PAGE *(When Data Entered)*

ABSTRACT (Box 20 cont.)

decreased the spray charge. Increasing the fluid pressure increased the total spray current, but not the charge-to-mass ratio. The greatest charge-to-mass ratio will be achieved with narrow-cone-angle nozzles.

X77-01

ELECTROSTATIC INDUCTION PARAMETERS TO ATTAIN MAXIMUM SPRAY CHARGE

By

John W. Carroz and Patrick N. Keller
Naval Weapons Center
China Lake, California

ABSTRACT

Laboratory experiments using sprays of charged drops were conducted to support a fog clearing program. Sprays from 1-gram per second hollow-cone industrial spray nozzles were induction-charged to 5.7×10^{-6} coulombs per gram of spray. As the nozzle size was increased, the charge per unit mass of spray decreased. Increasing the airflow past the nozzle increased the charge on the spray. Increasing induction surface, fluid conductivity, and voltage increased the spray charge to a limit beyond which further increases decreased the spray charge. Increasing the fluid pressure increased the total spray current but not the charge-to-mass ratio. The greatest charge-to-mass ratio will be achieved with narrow-cone-angle nozzles.

INTRODUCTION

The collection of fog droplets by charged sand particles or water drops spread from an airplane was suggested in a SCIENTIFIC AMERICAN article in 1923 (author unknown). Numerous investigations into the generation and behavior of charged drops have been made in the fields of physics, cloud physics, air pollution, rocket propulsion, spray painting, and agricultural engineering. Physicists have investigated charged drops along with other electrostatic phenomena. Cloud physicists have investigated charged drops in connection with drop coalescence, lightning, cloud electrification, etc. Electrostatic precipitation is one of the principal means of pollution control and has been in use since 1908. Electrical propulsion with charged drops was one of several advanced rocket propulsion techniques investigated in the laboratory in the late 1950s; 80 coulombs per kilogram (C/kg) of di-octylphthalate was achieved in one rocket propulsion experiment. Electrostatic paint spraying wastes less paint and provides better coverage because the drops follow the lines of force in the electric field, and thus curl around and coat the sides and rear of the object being painted. Agricultural engineers charge sprays to reduce spray drift and to provide better coverage of the undersides of leaves.

The laboratory experiments described in this report were conducted at the Naval Weapons Center in the fall of 1974 to support a fog clearing program, particularly the portion of the program making use of charged drops to improve visibility in fog so that aircraft can land. The charged drops must be sufficiently large so that the terminal, gravitational, settling velocity of the drops is fast enough to cause the drops to fall to the ground in a few minutes. The fog droplets beneath the falling spray drops

are collected and carried to the ground by the drops. Uncharged drops are poor collectors of smaller droplets because the smaller droplets are pushed aside by the air flowing around the falling drops. Highly charged drops are effective collectors of smaller droplets. A large (e.g., 10^6 electrons) charge on a drop induces a dipole on a fog droplet; then, since the pole nearer to the charged drop is of opposite sign to the charge on the drop, there is a net force attracting the droplet to the drop.

In order to sweep out a large percentage of the fog droplets, with the small amount of liquid an aircraft can carry, it is desirable to spray drops within a narrow size range, because even with charged drops the geometrical cross-sectional area of all of the spray drops must be large enough to cover a substantial fraction of the horizontal cross-sectional area of the fog being cleared. Thus, a balance must be maintained in drop size. The drops must be large enough to settle quickly to the ground yet small enough to have a high surface-to-mass ratio.

In order to collect sufficient fog droplets, the sprayed drops must be highly charged, near the limit of electrostatic rupture of the liquid drop. Lord Rayleigh (1879) defined this limit; and the maximum charge a drop can have without rupture is known as the Rayleigh stability limit.

One common misconception about small charged drops is that the dielectric strength of the air surrounding the drop limits the maximum drop charge to a small fraction of the Rayleigh limit. For large spheres this is true. For drops smaller than a few hundred micrometers in radius, investigators have found measurements of the maximum drop charge to be within a few percent of the Rayleigh stability limit, and the charge on the drops not limited by corona or Townsend discharge. (Hendricks, 1962; Doyle et. al.1964; Abbas and Latham, 1967; Schweizer and Hanson, 1971). Schweizer and Hanson's experiments with positively charged drops of n-octanol with radii of 7- to 20-μm showed drop

breakup within 4% of the calculated Rayleigh stability limit.

After reviewing the literature, making necessary simplifying assumptions, and calculating the amount of spray, drop size, and drop charge required, existing spray systems were considered inadequate for our requirements. A tenfold increase in spray current was required.

Variables investigated were nozzle type, induction surfaces, voltage, fluid composition, fluid pressure, nozzle size, and airflow. Since most of these variables are interrelated, time did not allow a complete characterization of each relative to all of the others. This report covers the results of laboratory experiments on these variables and the effect of the variables on the charging of drops. Although each variable is discussed separately, it is often impossible to separate the one under discussion from the others because they are so interrelated.

BACKGROUND

In order to design a high performance induction charging system, it is necessary to relate the net charge density, system geometry, and source voltage. This relationship is determined by the differential equation

$$\nabla^2\Phi = \frac{\rho}{\varepsilon} \tag{1}$$

together with the boundary conditions

$$\nabla_T\Phi = 0 \tag{2}$$

$$\nabla_N\Phi = \frac{\rho_s}{\varepsilon} \tag{3}$$

where

Φ = electric potential function

$\nabla_T\Phi$ = tangential component of the electric field at the surface of the conducting bodies

$\nabla_N\Phi$ = normal component of the electric field at the surface of the conducting bodies

ρ = charge density

ρ_s = surface charge density

ε = permittivity of the space

Once $\nabla_N\Phi$ is found, ρ_s may be calculated.

$$\rho_s = \nabla_N\Phi\varepsilon \tag{4}$$

There is a constraint on $\nabla_N\Phi$ caused by arcing. This may be expressed as

$$V_{AB} = \int_A^B \nabla\Phi \cdot \vec{d\ell} < V_a \tag{5}$$

which says that the voltage between any two points A and B of a system must be less than the electric breakover potential (arcing limit), V_a. For a given system, V_a is a function of the system geometry and the condition of the surface involved.

For most of the drop-charging systems of interest, calculating the surface charge density of forming drops is extremely difficult because the boundary conditions are awkward and the right-hand side of Equation 1 must account for all space charge (i.e., the charges of the drops that have separated from the system but are still in the vicinity of the separating liquid).

Fortunately, just knowledge of the form of the boundary value problem helps in the design of optimal electric induction drop-charging systems. It can be seen from Equation 4 that the higher the value of the normal component of the electric field strength ($\nabla_N \Phi$) at the surface of interest, the greater will be the charge density on this surface.

Jet/Cylinder Charging System

A simple electric induction drop-charging system that lends itself to analysis (Hendricks, 1973) is that which charges a jet from a capillary tube. Such a system is shown in Figure 1. The analysis and solution of this problem are of interest because they lead to analysis of the induction charging of other nozzles.

In Figure 1 a jet of liquid from a capillary tube enters a concentric cylinder which serves as the induction surface. From the relation

$$Q = A^* \rho_s \qquad (6)$$

where Q is charge, A* is the surface area of the liquid upon which the charge is located, and ρ_s is the surface charge density, it follows

$$\frac{Q}{v} = \frac{A}{v} \rho_s \tag{7}$$

where v is the volume of the liquid associated with surface area A*.

Solving the associated boundary value problem for ρ_s using axial and radial symmetry and neglecting end effects yields

$$\rho_s = \frac{\varepsilon V_0}{a \ln b/a} \tag{8}$$

where a and b are the radius of the jet and the cylinder, respectively, and V_0 is the potential difference between the jet and the cylinder.

Combining Equations 7 and 8 yields

$$\frac{Q}{v} = \frac{A^*}{v} \rho_s = \frac{2\varepsilon V_0}{a^2 \ln b/a} \tag{9}$$

As the jet travels along the axis of the cylinder it breaks into drops. In order to calculate the charge on a drop, an assumption can be made that the volume which breaks off forms only one drop. Only finely tuned systems lend themselves to this treatment.

The charge per drop of liquid leaving the system may now be calculated as the charge per unit volume times the volume per drop. The maximum charge per unit volume of a coaxial jet cylinder charging system is

$$\left.\frac{Q}{v}\right|_{max} = \frac{2\varepsilon}{a^2 \ln b/a} \left. V_0 \right|_{max} \tag{10}$$

The greatest value V_0 may have is the arcing limit, V_a. If the arcing voltage can be assumed to be linearly related to the distance between a and b then

$$V_0\Big|_{max} = V_a = K(b-a) \tag{11}$$

where K is a constant of proportionality usually quoted as 10^6 V/m.

By substitution

$$\frac{Q}{v}\Big|_{max} = \frac{2\varepsilon K(b-a)}{a^2 \ln b/a} \tag{12}$$

From this expression it is seen that for a given value of a (jet size), the value of charge to volume increases as b increases. However, to keep Q/v constant as a increases, b must be increased rapidly. Equation 12 cannot be solved for b in terms of known functions, but by choosing various values of a and calculating b it is found that, as a increases, b must increase faster than a^2 to maintain constant Q/v.

Cone Nozzle Charging System

An analysis of the induction charging of spray from a cone nozzle is more complex than the preceding analysis of a jet. In cone nozzles the fluid is fed into a whirl chamber through tangential passages so that it acquires a rapid rotation. An orifice is placed on the axis of the whirl chamber, and the fluid exits in the form of a hollow conical sheet which then breaks up into drops. Figure 2 shows a cross-section of a system induction-charging spray from a cone nozzle. Here a torus is used as the induction surface. Even though the system has axial symmetry, analysis is difficult. The presence of the charged drops in the spray cannot be neglected. The highest electric field strength in the system may not be located where the conical sheet is breaking into drops. Depending on the geometry of the system, the highest field may be, for example, between the induction surface and the nozzle head or between the back side of the induction surface and charged drops passing near this surface.

In considering that part of the conical sheet where shattering is taking place, it is much more instructive to consider the charge per unit length of circumference of the cone before and after separation than to try to make an analysis based on the charge per drop because the latter is effectively incalculable. The charge before and after separation will remain the same.

Equation 7 applies, where A* is the outer surface of the rim of the cone where shattering of the cone is occurring and v is the volume of liquid associated with this area. The maximum charge-to-mass ratio may be written in terms of two factors:

$$\left.\frac{Q}{v}\right|_{max} = \left[\left.\frac{A^*}{v}\right|_{max}\right] \cdot \left.\rho_s\right|_{max} \qquad (13)$$

The factor $\left.\frac{A^*}{v}\right|_{max}$ is variable for cone nozzles. The problems of finding $\left.\rho_s\right|_{max}$ are much more difficult here than were those of the jet/cylinder example because here the shape of the maximizing induction surface is an unknown. In a real system the effects of the ambient air on the cone and drops cannot be neglected. The induction surface may affect the air, and thus the aerodynamic effects of the induction surface must be included in the problem. Even when the nozzles are sprayed in still air there is entrainment of the air near the cone and there is an aerodynamic effect of any induction surface placed near the cone. When the air is moving past the system (a desirable condition) the effect of the lee eddies of the induction surface become important, and the entire problem is then exceedingly difficult to analyze. It was decided to try to maximize ρ_s with respect to induction surface size, shape, placement, and airflow by laboratory experiments.

EXPERIMENTAL APPARATUS AND PROCEDURES

Because the charged spray was to be sprayed from an aircraft flying at 72 m/s (140 knots), the laboratory experiments were conducted in an airstream. Figure 3 shows the arrangement of the apparatus used for the majority of the tests. The water reservoir was insulated from the wooden supports, as were the microammeters and high-voltage supply. The case of the 110V AC-powered high-voltage supply was ungrounded by disconnecting the ground wire. A charge collector, consisting of a 55-gallon drum, screen, and plate, captured the spray's charge and was suspended 0.2 meter below the nozzle. Monofilament nylon fishing line was used for insulators. PVC pipe insulated the fan from the system. The fan was further separated from the other apparatus by a metal wall because the fan motor generated significant electrical noise. The nozzle and charged induction surface were placed inside the PVC pipe so that the air blown by the fan, at about 50 m/s at maximum fan output, would rush by them. The 5.1-centimeter ID PVC pipe was straight for over 40 pipe diameters upstream from the nozzle. Figure 4 shows a schematic of the electrical setup. Moving coil microammeters were used to measure the spray current and the induction surface leakage. The high-voltage power supply was adjustable up to 30 kilovolts.

When experiments were conducted, the induction surface leakage would increase as the induction surface was wet by the spray, which was swirled in the turbulent air above the charge collector. Initial and steady state readings were taken. Two water reservoirs were used, one a 75-liter stainless steel tank (shown in Figure 3) which could be pressurized to 0.86 megapascal (MPa) (125 psi) and a 1-liter stainless steel bottle (not shown) which could be pressurized to 3.4 MPa (500 psi).

The experiment was sensiti[illegible] to the water reservoir used, [illegible] current being 15% lower when the 1-liter bottle was used. The experimental values also varied for unknown reasons from day to day by about ±5%.

EXPERIMENTAL RESULTS*

INDUCTION SURFACES

Rings and tori were used as the induction surfaces for induction-charging sprays. Tori were made by bending small-diameter copper tubing and soldering the end (Figure 5a); the rings were made by cutting off short pieces of larger-diameter copper tubing or pipe (Figure 5b).

Induction surfaces directly in the path of the spray arced to the nozzle at field strengths less than those required to induce high spray currents. Even when the spray did not strike the surfaces directly, they were wet by drops carried in eddies in the airflow exiting from the pipe. This was not an experimental deficiency because the most practical designs of the induction surfaces and nozzle supports result in air turbulence with surface wetting by the spray. When the equipment is flown in fog, the fog droplets will also wet the hardware.

Three sizes of tori were tested. The smallest size had a major diameter of 2.2 centimeters and a minor diameter of 0.64 centimeter and was large enough to be used with all of the 30-degree cone nozzles tested. The tori were mounted coaxially with the nozzle tip (See Figure 2). The smallest-size torus induced the maximum net charge.

Those tori with larger inside diameters required higher voltages to create a given electric field strength at the nozzle and to attain a corresponding value of net spray charge. In general there is less corona

*Unless otherwise stated, the experiments were conducted with 30-degree hollow-cone, stainless steel, nozzles manufactured by Steinen Co. and donated by Electro Gas Dynamics Inc. The fluid pressures are listed as gauge pressures.

emitted from the smaller-diameter induction surfaces with their corresponding lower voltages, so the maximum attainable net charge on the spray is greater. The smaller sizes of similar shapes have less surface area to catch liquid and to emit charged drops of the sign opposite to that of the induced charge on the spray. When spray was being induction-charged, drops of liquid as large as 6 millimeters in diameter could be seen on the conductor. The drops were cone-shaped, and small charged drops were emitted from the sharp point of the apex.

A ring, 2.54 centimeters high with an inside diameter of 2.54 centimeters, gave the best results. There was usually less corona loss from the smallest-size torus so the net charge on the spray was usually greater than when the ring was used.

FLUID COMPOSITION

The initial experiments were conducted with distilled water with a conductivity of (4×10^{-4} siemens/m). When water with this low conductivity (and thus long charge relaxation time) and a nominal 1-g/s hollow-cone nozzle were used, the current on the spray did not increase as the fluid pressure was increased from 0.7 to 2.1 MPa (100 to 300 psi) (Figure 6). The low conductivity of the distilled water is not sufficient to allow the charge to flow from the extended liquid back to the nozzle at the higher pressures, because the liquid breaks into drops after exiting from the nozzle in less time than at lower fluid pressures. When China Lake tap water or any of several ion-producing substances were added to the distilled water, the current rose as the pressure was increased.

Jarvis (1972) studied the effect of various salts on the surface potential. In order to investigate the possibility that sprays of some solutions could be charged higher positively and others negatively, the following amounts of material were added to 1 kilogram of distilled water: 10 drops of concentrated NH_4OH; 0.25×10^{-3} kg NaCl; 5×10^{-3} kg urea; 0.1 kg urea; 21×10^{-3} kg Na_2SO_4; 0.06 kg $MgSO_4$. The instrument used to measure conductivity would not measure conductivities in excess of 1.3 siemens/m; thus conductivities of some high-salt-content solutions also tested were not measured. The conductivities of these solutions can be determined to within about 10% by using Lange's Handbook Chemistry (1956). Figure 7 shows the maximum current obtained using nominal 3-g/s hollow-cone nozzles operating at a solution pressure of 1.4 MPa. Figure 8 shows the maximum current obtained while operating at 2.1 MPa. The +'s are for a positively charged induction surface; the -'s for negative. With one exception it was always possible to induce a larger negative charge onto the spray with a positively charged induction surface than it was to induce a positive charge with a negatively charged surface. The exception was with $MgSO_4$ solutions, which had the opposite result. Based on the few tests conducted, the maximum total charge on the spray appeared to be determined primarily by the solution's conductivity rather than the material used to raise the conductivity.

FLUID PRESSURE

For a given nozzle the median spray drop size decreases with increasing pressure. In order to spray a given median drop size at a higher flow rate, a larger-size nozzle can be used if the operating pressure is increased. Dr. R. W. Tate, Director of Research at Delavan Manufacturing Company, has stated that when spraying water a Delavan WDA 3.0 (nominal 3-g/s) 80-degree nozzle sprays a 92-μm Sauter mean diameter at 0.7 MPa and a 67-μm Sauter mean diameter at 2.1 MPa.* A nominal 1-g/s Delavan nozzle sprays a 70-μm Sauter mean diameter at 0.7 MPa. The spray from Steinen nozzles should have similar characteristics.

*Personal communication

Figure 9 shows the current per 3-g/s nozzle versus pressure for a conductive solution of 0.06 kg of $MgSO_4$ per kg of water. As shown in Table 1, while the current flowing out on the spray was greater for the higher pressure, the charge per unit mass was the same because the flow rate went up as much as the current. There was a smaller fraction of the Rayleigh charge on the drops at the higher pressure because the drop sizes were smaller.

TABLE 1. Comparison of Flow Rate, Current, and Charge per Unit Mass at Various Fluid Pressures.

Nominal 3-g/s hollow-cone nozzle, 0.06 kg $MgSO_4$ per kg of water, and positively charged induction surface.

Item	Pressure, MPa		
	1.4	2.1	2.8
Fluid flow rate, g/s. . . .	3.2	3.9	4.5
Spray current, μA	9.1	11.5	13
Charge per unit mass, C/g .	2.8×10^{-6}	2.9×10^{-6}	2.9×10^{-6}

VOLTAGE

The spray charge is dependent upon the voltage on the induction surface. At first the net spray charge rises as the voltage increases; it then peaks and falls rapidly as the voltage is increased further.

As the voltage on the induction surface increases, more charge of the sign opposite to that of the induction surface is induced onto the spray. At the same time, as the voltage increases, more charged drops of the same polarity as the induction surface are emitted by corona discharge from conical-shaped liquid drops on the wet induction surface. As the voltage on the induction surface is raised higher, the electric field in the air surrounding the induction surface generates light ions. The current flow of light ions rises rapidly as the field approaches the breakdown strength of air.

The voltage at which the highest net current was flowing from the nozzle to the charge collector varied for each nozzle, induction surface, and solution. Higher voltages increased the corona production of charged particles emitted from wet induction surfaces. The maximum net currents were noted at lower voltages as a dry induction surface became wet. Thus, there is a maximum voltage to which the induction surface should be raised to produce the largest net current; higher voltages result in a decrease in net current.

The voltage at which arcing occurs between the induction surface and the nozzle depends upon the size of the air gap between them, the airflow, the spray cone angle, and the conductivity of the liquid being sprayed. Since induction surfaces with minimum inside diameter perform satisfactorily at lower voltages, they do not have any greater tendency to spark than the surfaces with larger inside diameter. Higher airflows allow a higher voltage without sparking. A narrow-angle spray which did not strike the induction surface was superior. Water solutions having high electrical conductivities or viscosities caused sparking

problems. Viscous, conductive liquids do not spray well and form legaments which can act as an electrical short if they extend between the nozzle and induction surface. A reduction of 38% in the spark-over voltage was observed for $MgCl_2$ (0.45 kg per kg of water).

The results consistently showed slightly higher net currents when the induction surface was charged positively than when it was charged negatively (Figure 7). This difference between positive and negative is to be expected because the properties of positive and negative ions are different (Thomson and Thomson, 1928).

NOZZLE SIZE

The nozzle size had an effect on the charge-to-mass ratios. Tests with smaller nozzles usually resulted in larger ratios of spray currents to flow rates. Spraying distilled water of 7.4×10^{-4} siemens/m conductivity at 0.7 MPa resulted in a rather constant charge-to-mass ratio; the maximum current flowing out on the spray was 2.7 microamperes (μA) for a 1-g/s solid-cone nozzle (3×10^{-6} C/g), 5.3 μA for a 2-g/s hollow-cone nozzle (2.9×10^{-6} C/g), and 6.9 μA for a 3-g/s hollow-cone nozzle (2.6×10^{6} C/G). When distilled water of 4×10^{-4} siemens/m conductivity was sprayed at 0.7 MPa from the 1-g/s solid-cone nozzle, the maximum current flowing out on the spray was 2.1 μA.

A nominal 1-g/s hollow-cone nozzle spraying conductive solution (0.36 kg of $MgSO_4$ per kg of distilled water) at 2.1 MPa resulted in 1.3 g/s of spray and 7.4 μA of current flowing out on the spray (5.7×10^{-6} C/g). With a 3-g/s nozzle, the solution contained only 0.06 kg of $MgSO_4$ per kg of water, so unfortunately, the following comparison is somewhat suspect. With the 3-g/s hollow-cone nozzle also spraying at 2.1 MPa, the current was 11.5 μA (2.9×10^{-6} C/g).

With the 3-g/s nozzle spraying a solution of 5×10^{-3} kg of NaCl per kg of water at 2.1 MPa, the maximum current was 12.7 μA. With a 10-g/s nozzle, spraying the same solution at the same pressure, the maximum current was 17 μA. Figure 10 shows the maximum current per nozzle and the current-to-mass ratios for the 1-, 3- and 10-g/s nozzles spraying conductive solutions at 2.1 MPa.

Fig 10

OTHER NOZZLES

A variety of other pressure nozzles were tested: flat spray pattern nozzles (Spraying Systems Co., Teejet Nozzles, Numbers 2515 and 8015), pin jet nozzles* (Bete Fog Nozzle Inc., Nozzle Number P-40 and Spraco, Nozzle Number 1507), and some cone nozzles with spray cone angles larger than 30°. Also tested were two pneumatic atomizing nozzles, one with a wide angle round spray pattern, another with a narrow angle round spray pattern (Spraying Systems Co., Nozzle Numbers 2050/67-6-20-70° and 2850/73160 respectively). In the experiments the charge-to-mass ratios were highest when the 30-degree cone nozzles were used.

AIRFLOW

Tests were conducted in the NWC wind tunnel at airspeeds from 51 to 74 m/s. The spray current increased as the airflow increased. In these wind tunnel tests with three nozzles positioned 3.5 centimeters apart, the spray current increased from 38 μA at an air velocity of 51 m/s to 45 μA at 74 m/s.

The electric field associated with the cloud of charged drops opposes the field from the charged conductor. As the airflow increases, the cloud of charged drops moves away from the nozzle faster, diminishing this opposing field and allowing a higher spray current. The nozzles used in the wind tunnel tests were 3-g/s, Delavan 30-degree, brass, hollow-cone nozzles. Their flow rate at 2.1 MPa pressure was 4.2 g/s per nozzle.

*In pin jet nozzles the liquid passes through an orifice and impacts onto the flat end of a pin positioned down stream of the orifice.

DISCUSSION OF RESULTS

For cone nozzles the surface-to-volume ratio of the rim at the breaking edge of the conical sheet is

$$\frac{A^*}{v} = \frac{2\bar{a}\pi L}{2\bar{a}\pi Lt} = \frac{1}{t} \qquad (14)$$

where $\bar{a}$ is the average radius of the rim, L is the axial length of the rim, and t is the rim thickness. By measurements of the electrical resistance from the nozzle head to a probe in the spray, we were able to determine the approximate location of the breaking edges of spray cones. We observed that the diameter of the cone at the breaking edge increases slowly as the size (in terms of flow rate) of the nozzle increases. If the fluid velocities in the cones from nozzles of different sizes, all operating at the same pressure, are assumed to be equal (fluid velocity assumed proportional to drop in fluid pressure across the nozzles), this implies that the thickness of the cones increases as the nozzle size increases. Equation 14 then implies that small size nozzles will give a superior charge-to-volume ratio. The measurements of cone diameter at the breaking edge were made only on commercial nozzles, but they did not seem to vary much from one manufacturer to another. The factors governing the minimum t a cone nozzle may have for a given flow rate are unknown to us, but attempts to minimize t by polishing the nozzle throat and whirl chamber and by using guar gum in the fluid failed to improve the charge-to-volume ratio.

The reason narrow-angle nozzles charge better than wide-angle nozzles is twofold. First, with the wide-angle cones, many very small drops hit the induction surface because more of the spray passes into the

turbulence behind the induction surface. This results in the formation of many drops on the induction surface, each of which can produce corona discharge. The net spray current is lowered because ions and very small drops emitted from the wet induction surface are of opposite polarity to the induced charge. The second reason can be seen from Equation 13. We found again by resistance measurements that the diameters of the breaking edges of the cones do not vary significantly with cone angles. If the fluid velocities in the cones are assumed to be approximately equal, this implies that t does not vary significantly with nozzle angles. Thus, the factor A^*/v_{max} in Equation 13 is approximately invariant with changes of nozzle angle. For a very-narrow-angle nozzle it is reasonable to expect $\rho_{s\ max}$ to behave like $\rho_{s\ max}$ of the jet-charging system (Equation 8), which has no theoretical limit. At cone angles approaching 180 degrees, $\rho_{s\ max}$ will approach $\rho_{s\ max}$ of two flat plates, which is $K\varepsilon$ and is a fixed limit. Thus, with the stipulation that the factor A^*/v_{max} does not change, narrow-angle nozzles should tend toward the theoretically unbounded charge-to-mass ratio and thus be capable of higher charge-to-mass ratios than wide-angle nozzles.

The main reason that the drop charges were so much higher in our experiments than in the induction charging experiments of Law and Bowen (1966) was that high velocity air flowed past the induction surface and nozzle in our experiments. Splinter (1968) used high (32 m/s) airflows while induction-charging a 5-g/s hollow-cone nozzle and achieved high drop charges; the maximum nozzle spray current was 8 μA with +15 kilovolts on the induction surface and with a fluid flow rate of 4-g/s of water at 0.47 MPa. The maximum spray charge was 1.9×10^{-6} C/g, which is almost

as high as we achieved with the 3-g/s, 2.1-MPa tests. Splinter reported large decreases in the spray current for conductive water (2.5×10^{-3} kg of NaCl per kg of water) while corona-charging the spray. He did not report results of induction-charging conductive water. When induction-charging, we found that the conductivity of the liquid being sprayed was important and, for each nozzle, there was a pressure, above which adding salts to distilled water significantly increased the spray current.

The laboratory testing resulted in a large increase in the spray current per nozzle compared to the setup used in prior fog clearing experiments. The spray current from a 3-g/s nozzle spraying slightly salty water at 2.1 MPa was 4.6 times as great as the spray current from a 1-g/s nozzle spraying distilled water at 0.7 MPa. The fog clearing capacity of a nozzle is dependent upon the drop charge and the total geometrical cross section of those drops in the spray which are large enough to fall through the fog fast enough for the particular operating conditions. Since the drop-size distribution of the 3-g/s nozzle at 2.1 MPa is close to that of the 1-g/s nozzle at 0.7 MPa, the difference in flow rates between the nozzles (3.8 versus 1-g/s) is also a measure of the difference in relative spray cross section areas; therefore, the geometrical cross section of the spray from the 3-g/s nozzle is about 3.8 times that of the 1-g/s nozzle.

CONCLUSIONS

It is possible to charge sprays up to 5.7×10^{-6} C/g by the proper choice of nozzle, induction surface, fluid composition, fluid pressure, voltage, nozzle size, and airflow. The highest charge per unit mass of spray is achieved with the lowest flow rate and the highest airflow. Increasing induction surface, fluid conductivity, and voltage increases the spray charging up to a point, then further increases are detrimental. Increasing fluid pressure increases the total spray current but not the charge-to-mass ratio.

REFERENCES

1 Abbas, M. A., and J. Latham. 1967. The instability of evaporating charged drops. J. FLUID MECH 30:663-70.

2 Doyle, A., D. R. Moffett, and B. Vonnegut. 1964. Behavior of evaporating electrically charged droplets. J. COLLOID SCI 19:136-43.

3 Hendricks, C. D. 1962. Charged droplet experiments. J COLLOID SCI 17: 249-59.

4 Hendricks, C. D. 1973: Charging macroscopic particles. pp. 57-85. In: A. D. Moore, (Ed.). Electrostatics and its applications. John Wiley and Sons, New York.

5 Jarvis, N. L. 1972. Effect of various salts on the surface potential of water-air interface. J GEOPHYS RES 77(27):5177-82.

6 Lange, N. A. 1956. Handbook of chemistry. Handbook Publishers, Inc., Sandusky, Ohio. pp. 1206-1211.

7 Law, S. E., and H. D. Bowen. 1966. Charging liquid spray by electrostatic induction. TRANSACTIONS of the ASAE 9(4):501-506.

8 Raleigh, Lord. 1879. On the equilibrium of liquid conducting masses charged with electricity. PROC ROY SOC:184-186.

9 Schweizer, J. W., and D. N. Hanson. 1971. Stability limit of charged drops. J COLLOID AND INTERFACE SCI 35(3):417-23.

10 Splinter, W. E. 1968. Electrostatic charging of agricultural sprays. TRANSACTIONS of the ASAE 11(3):491-495.

11 Thomson, J. J., and G. P. Thomson. 1928. Conduction of electricity through gases. Vol. 1. Dover Publications, Inc., New York. 391 p.

12 Unknown author. 1923. Sand-blasting the clouds for man-made weather. SCI AMER 128:224.

FIGURES

TABLE

TABLE 1. Comparison of Flow Rate, Current, and Charge per Unit Mass at Various Fluid Pressures.

Nominal 3-g/s hollow-cone nozzle, 0.06 kg $MgSO_4$ per kg of water, and positively charged induction surface.

Item	Pressure, MPa		
	1.4	2.1	2.8
Fluid flow rate, g/s. . . .	3.2	3.9	4.5
Spray current, μA	9.1	11.5	13
Charge per unit mass, C/g .	2.8×10^{-6}	2.9×10^{-6}	2.9×10^{-6}

Figure 1

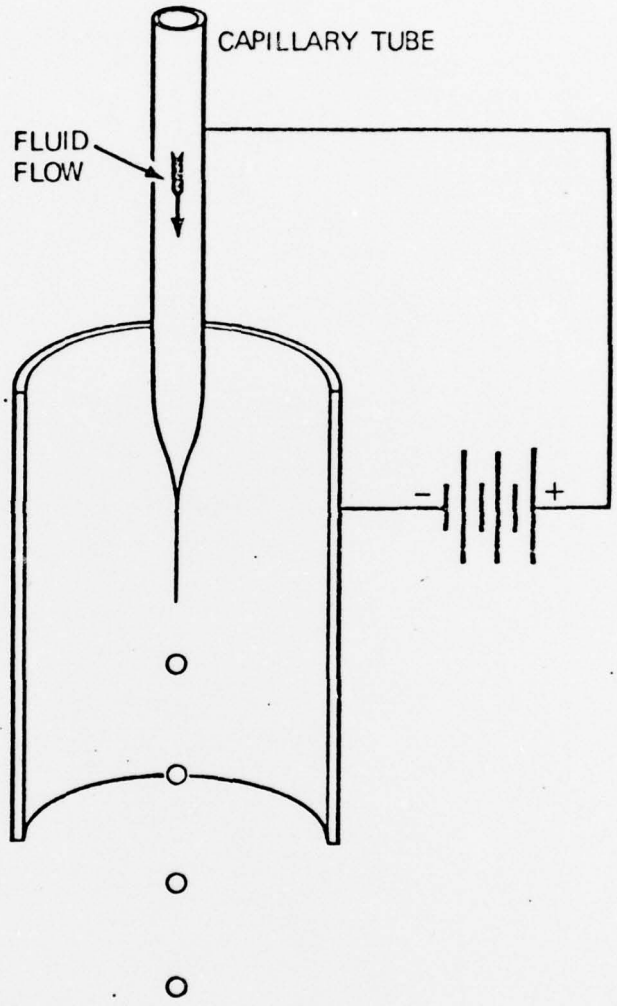

Figure 2

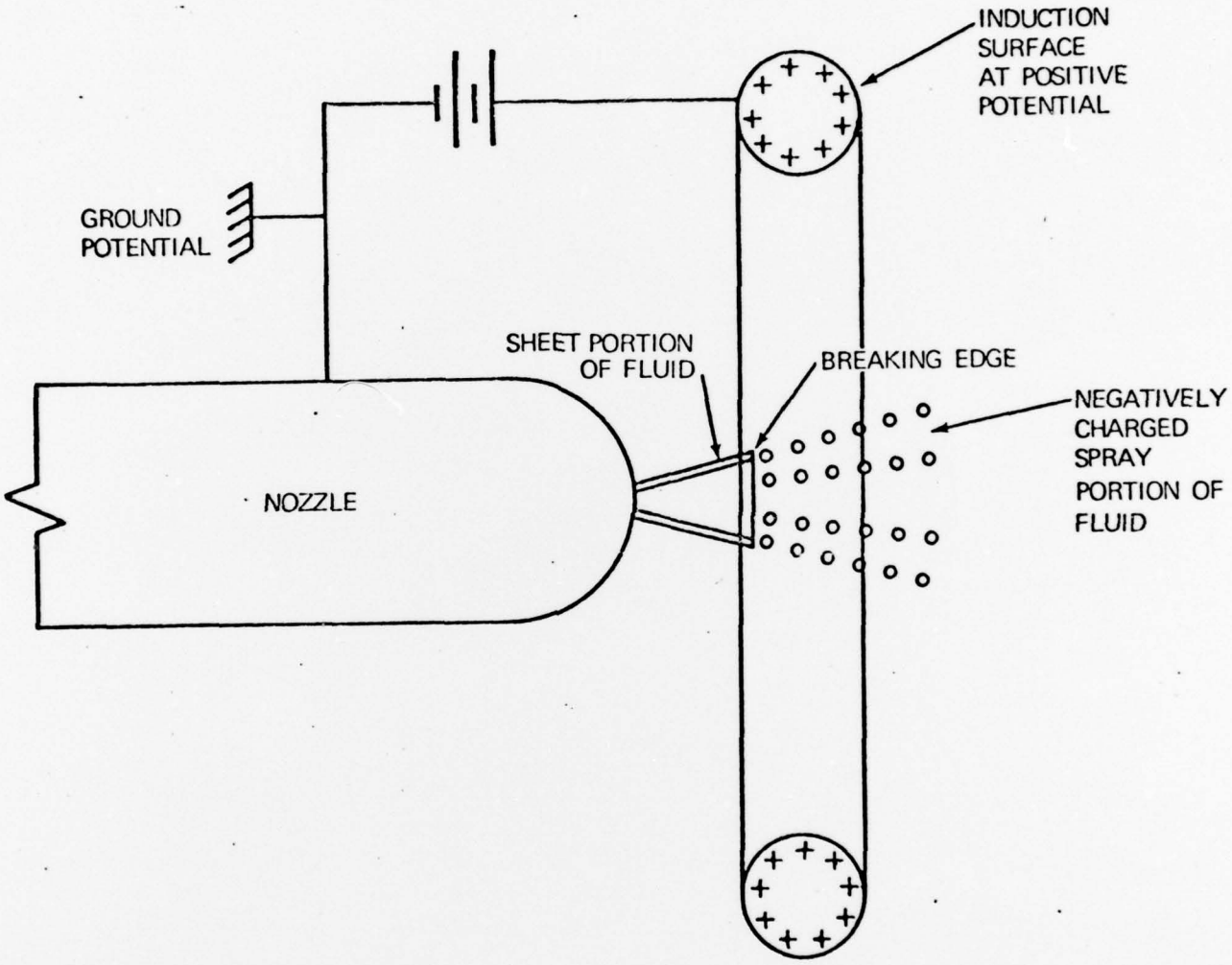
INDUCTION
SURFACE
AT POSITIVE
POTENTIAL
GROUND
POTENTIAL
SHEET PORTION
OF FLUID
BREAKING EDGE
NEGATIVELY
CHARGED
SPRAY
PORTION OF
FLUID
NOZZLE

Figure 3

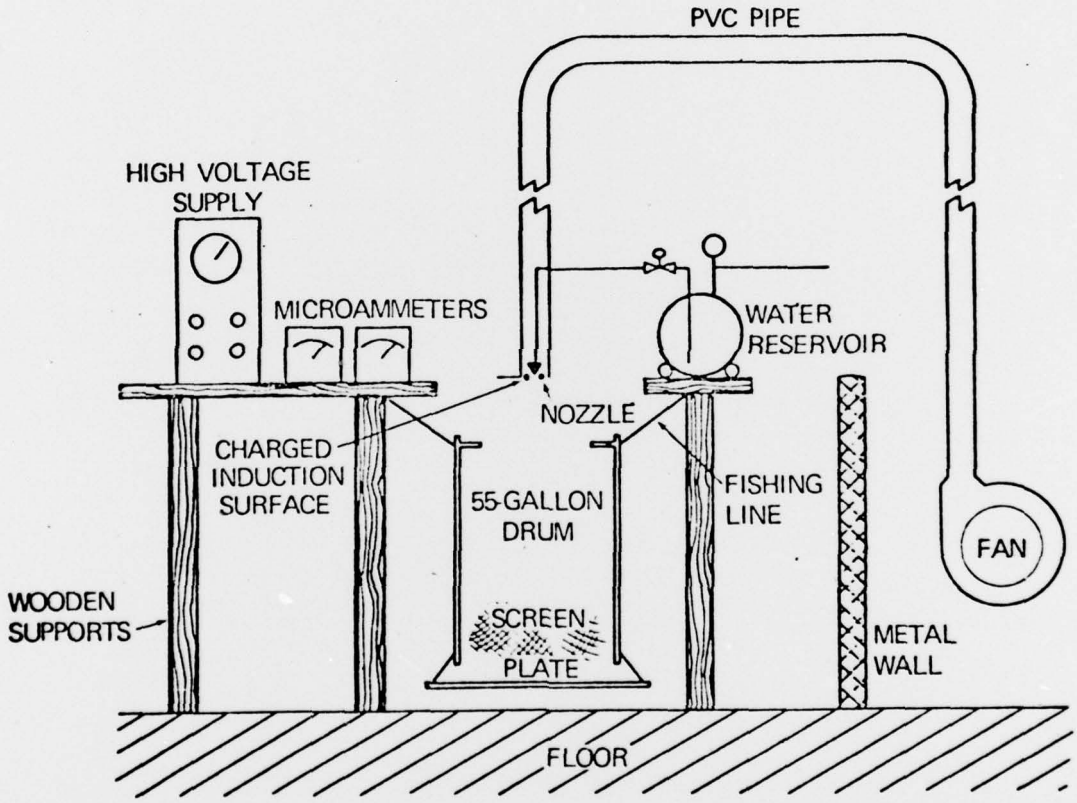
PVC PIPE
HIGH VOLTAGE SUPPLY
MICROAMMETERS
WATER RESERVOIR
NOZZLE
CHARGED INDUCTION SURFACE
55-GALLON DRUM
FISHING LINE
FAN
WOODEN SUPPORTS
SCREEN
PLATE
METAL WALL
FLOOR

Figure 4

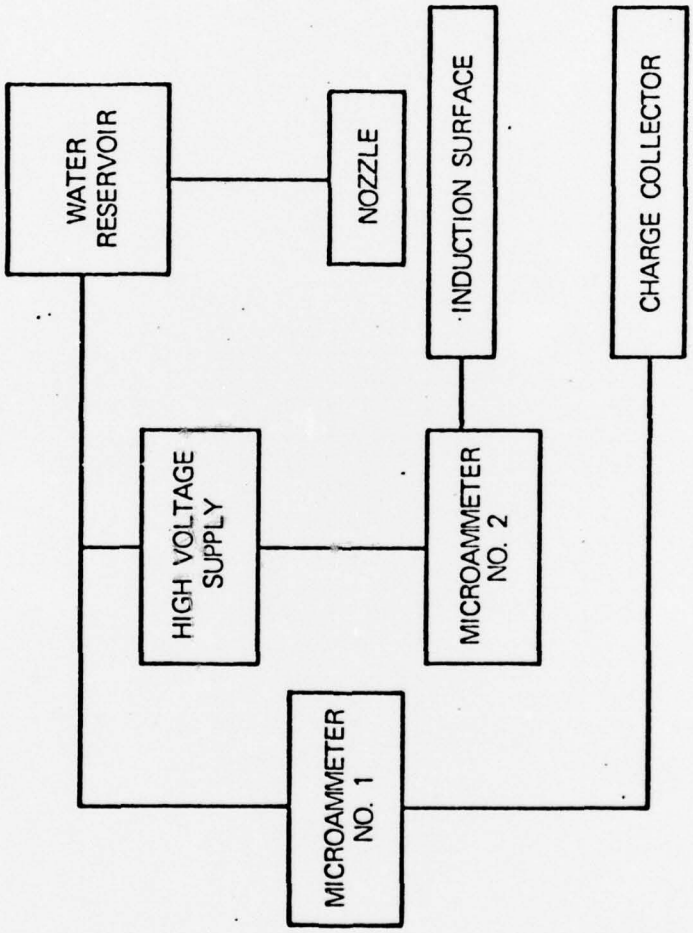
WATER RESERVOIR
NOZZLE
INDUCTION SURFACE
CHARGE COLLECTOR
HIGH VOLTAGE SUPPLY
MICROAMMETER NO. 2
MICROAMMETER NO. 1

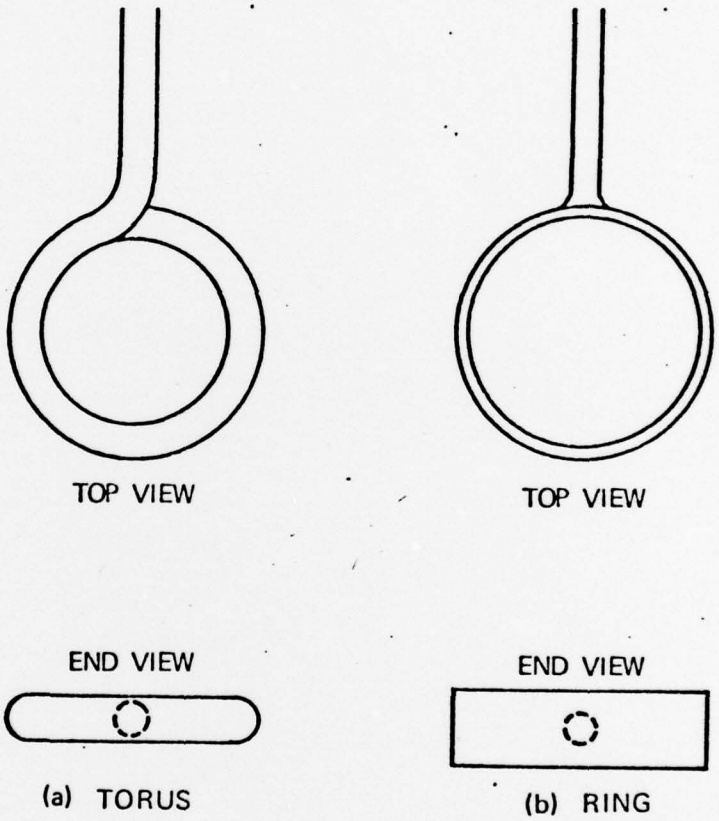
TOP VIEW
TOP VIEW
END VIEW
END VIEW
(a) TORUS
(b) RING

Figure 6

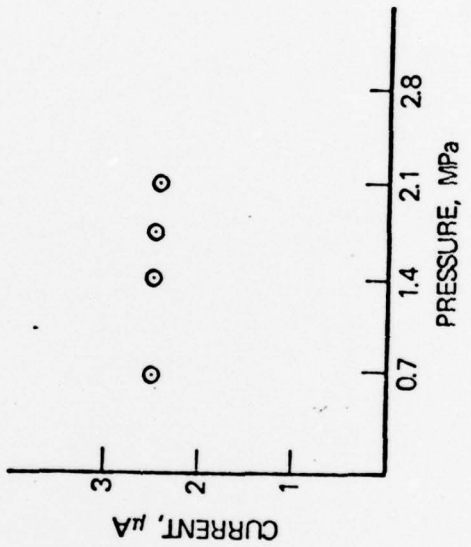

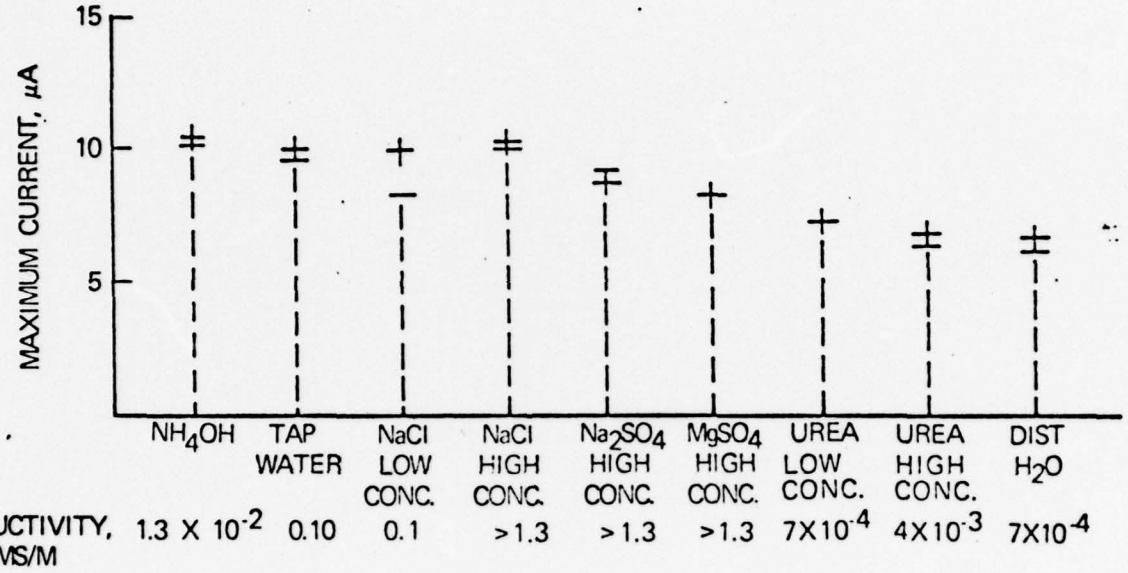
MAXIMUM CURRENT, μA
15
10
5
NH4OH
TAP WATER
NaCl LOW CONC.
NaCl HIGH CONC.
Na2SO4 HIGH CONC.
MgSO4 HIGH CONC.
UREA LOW CONC.
UREA HIGH CONC.
DIST H2O
CONDUCTIVITY, SIEMEMS/M
1.3 X 10-2
0.10
0.1
>1.3
>1.3
>1.3
7X10-4
4X10-3
7X10-4

Figure 1

Figure 8

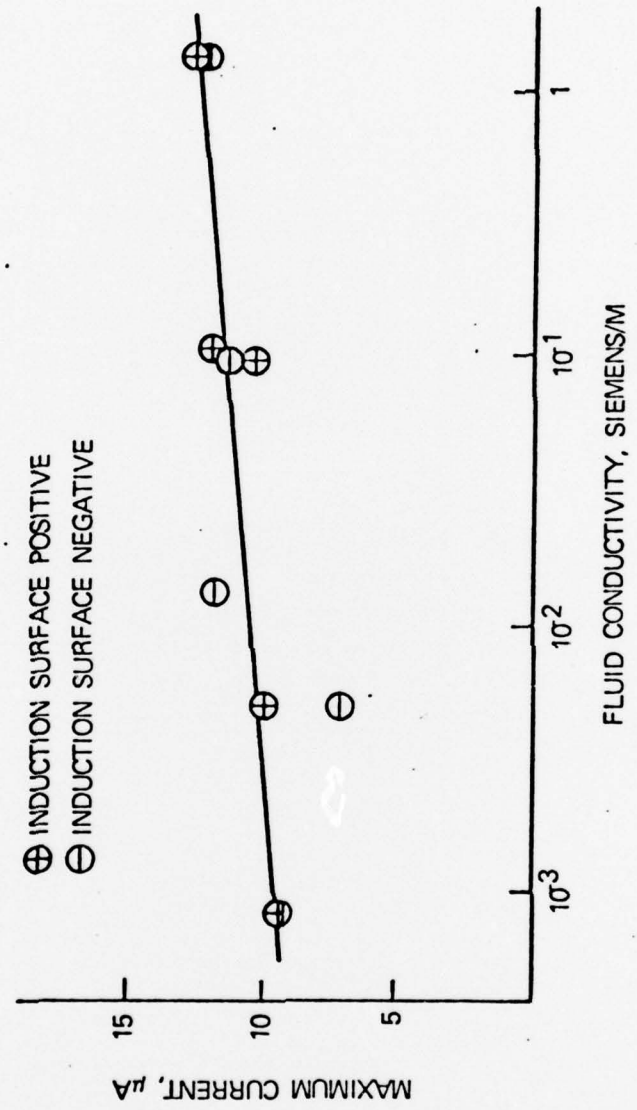
⊕ INDUCTION SURFACE POSITIVE
⊖ INDUCTION SURFACE NEGATIVE
MAXIMUM CURRENT, μA
15
10
5
10^{-3}
10^{-2}
10^{-1}
1
FLUID CONDUCTIVITY, SIEMENS/M

Figure 9

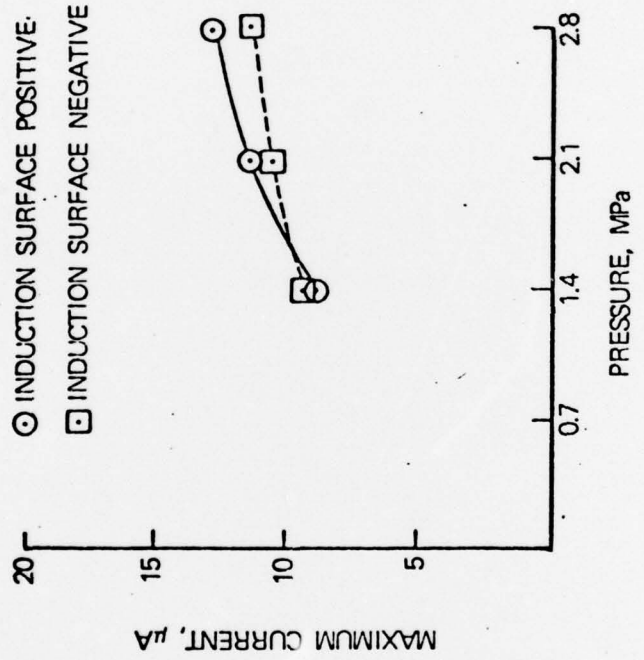
⊙ INDUCTION SURFACE POSITIVE
⊡ INDUCTION SURFACE NEGATIVE
MAXIMUM CURRENT, μA
20
15
10
5
0.7
1.4
2.1
2.8
PRESSURE, MPa

Figure 10

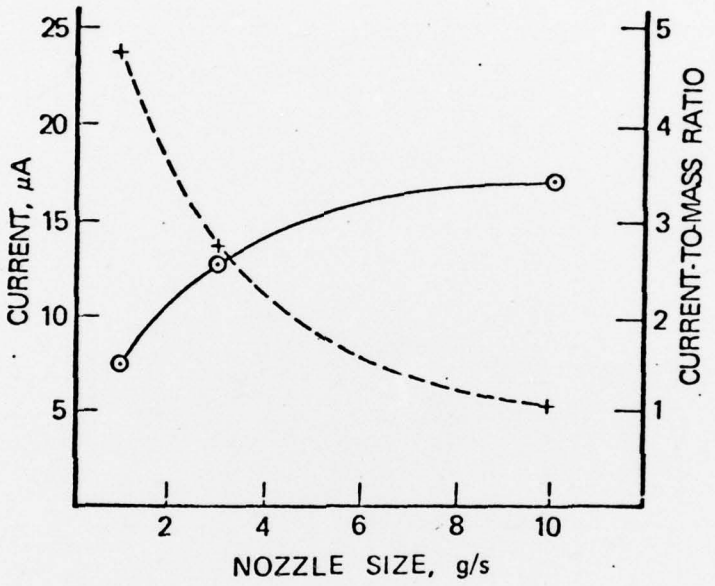
25
20
15
10
5
CURRENT, μA
5
4
3
2
1
CURRENT-TO-MASS RATIO
2
4
6
8
10
NOZZLE SIZE, g/s